Proceedings of ICRC 2001: 1 © Copernicus Gesellschaft 2001

ICRC 2001

WIMPs Are Stronger When They Stick Together

A. V. OLINTO[1,3], P. BLASI[2,3], and C. TYLER[1]

[1]Department of Astronomy & Astrophysics, & Enrico Fermi Institute, The University of Chicago, Chicago, IL 60637
[2]Fermi National Accelerator Laboratory, Batavia, IL 60510-0500
[3]Arcetri Osservatorio, Firenze, Italia

Abstract. Weakly interacting massive particles (WIMPs) remain the strongest candidates for the dark matter in the Universe. If WIMPs are the dark matter, they will form galactic halos according to the hierarchical clustering observed in N-body simulations. Cold dark matter (CDM) simulations show that large dark matter structures such as galactic and cluster halos are formed by the merging of many smaller clumps of dark matter. Each clump or halo is characterized by a centrally cusped density profile that can enhance the rate of WIMP annihilation and make the annihilation products more easily detectable. Electrons and positrons generated as decay products of WIMP annihilation emit synchrotron radiation in the Galactic magnetic field. We study the synchrotron signature from the clumps of dark matter in our Galactic halo. We find that the emission in the radio and microwave region of the electromagnetic spectrum can be above the CMB anisotropy level and should be detectable by CMB anisotropy experiments. Depending on the density profile of dark matter clumps, hundreds of clumps can have detectable fluxes and angular sizes.

1 Introduction

The density of dark matter in the present Universe is observed via its gravitational effects on galaxies and clusters of galaxies to constitute at least about 30% of the critical density of the Universe, but the nature of this dark matter is still unknown. Primordial nucleosynthesis constrains the density of baryonic matter to be less than about 5% of the critical density, thus most of the dark matter is non-baryonic. The leading candidate for the dark matter is the lightest supersymmetric particle in supersymmetric extensions of the standard model that is stable by conservation of R-parity. In most scenarios this weakly interacting massive particle (WIMP) is the neutralino, χ (for a review, see Jungman, Kamionkowski and Griest (1996)).

Correspondence to: olinto@oddjob.uchicago.edu

Neutralinos may be detected directly as they traverse the Earth or indirectly by the observation of their annihilation products. Direct neutralino searches are now underway in a number of low temperature experiments with no consensus detection as of yet. Indirect searches have been proposed both for gamma rays and synchrotron emission from the annihilation of WIMPs in the Galactic center (Berezinsky, Gurevich, and Zybin, 1992; Berezinsky, Bottino, and Mignola, 1994) where the WIMP density and magnetic field around a central massive black hole may enhance the emission significantly (Gondolo and Silk, 1999; Gondolo, 2000). The rate of annihilation is proportional to the neutralino density squared ($\sim n_\chi^2$), therefore the strongest flux is expected to come from the Galactic center where the dark matter halo density peaks.

N-body cold dark matter (CDM) simulations have shown that the dark matter halos have a density profile with a cusp at the center (within a core radius $R_c \sim 5-10$ kpc) and a steeper profile in the outer regions. The slope of the inner cusp is still a matter of debate ranging from r^{-1} to r^{-2} in different simulations. Superimposed on the smooth component, the high-resolution simulations find a large degree of substructure formed due to the constant merging of smaller halos to form the present dark matter halo (see, for example, Ghigna et al. (1998)). The large number of clumps generated through the hierarchical clustering of dark matter comprise about $\sim 10-20\%$ of the total mass and can enhance significantly the emission of gamma rays and neutrinos from neutralino annihilation in higher density clumps (Bergström et al., 1999; Calcáneo–Roldán and Moore, 2001). We show here (and in more detail in Blasi, Olinto and Tyler (2001)) that the synchrotron radiation of electrons and positrons generated as decay products of WIMP annihilation in the Galactic magnetic field can provide a crucial test of WIMP models, since the predicted fluxes are in the microwave region and exceed the signal of CMB anisotropies at some frequencies. The detection of this excess radiation from small angular size regions in the sky may provide the first signal from WIMP annihilations.

2 Synchrotron Signature of WIMP Clumps

The annihilation of neutralinos produces high energy particles through several processes, depending on the mixture of supersymmetric fields that form the neutralino. In addition to the gamma ray line generated in the channel $\chi\bar{\chi} \to \gamma\gamma$, the annihilation of two neutralinos also results in a continuum of particles (gamma rays, neutrinos, electrons, positrons, muons, etc.) that have energy spectra well represented by an $E^{-3/2}$ power law. This is typical of the process of fragmentation and hadronization of quarks into hadrons (mainly pions) and their decay into secondary products. Here we concentrate on the process $\chi\bar{\chi} \to q\bar{q} \to$ hadrons and the decay of the resulting pions. (We neglect the small contribution from kaons and other mesons.) In particular, we are interested in the e^+e^- pairs generated by the decay of the charged pions.

When the annihilation of neutralinos occurs in the Galaxy, the secondary products are injected in the ambient magnetic field. Clumps can be brightened by the synchrotron emission of e^+e^- pairs in the Galactic field, depending on their position in the halo.

We initially assume that the electrons emit in the same region in which they are generated, which is the case when $e^\pm$ are magnetically constrained in the higher magnetic field regions. As the field decays, the diffusion of the emitting $e^\pm$ needs to be included (see Blasi, Olinto and Tyler (2001)).

The spectrum of the generated $e^\pm$ naturally cuts off at about the neutralino mass, m_χ. Therefore, the relevant frequency range for $e^\pm$ synchrotron emission lies below the maximum frequency,

$$\nu_{\max} \simeq B_\mu (m_\chi/100\,\mathrm{GeV})^2\,\mathrm{GHz}\,, \tag{1}$$

where $B_\mu = B/\mu$G. Since the Galactic magnetic field is around μG, for $m_\chi \gtrsim 100$ GeV, the radiation will extend up to microwave frequencies. Note that the electron-positron spectra are flatter than E^{-2} which implies that most of the energy is carried by the most energetic $e^\pm$ particles, and most of the synchrotron emission occurs at frequencies approaching the cutoff.

In our calculations, we assumed that the Galactic magnetic field has an exponential scale height as in Stanev (1997). To model the smooth halo component, we considered the NFW halo profile (Navarro, Frenk and White, 1996, 1997)

$$\rho_{\rm halo} = m_\chi n_0 \left(\frac{r}{r_c}\right)^{-1} \left[1 + \frac{r}{r_c}\right]^{-2}\,, \tag{2}$$

where r_c is the core radius and n_0 is the number density at r_c. The two parameters, r_c and n_0, can be set by requiring that the halo contains a given total mass (M_H) and that the velocity dispersion at some distance from the center is known (in the case of the Galaxy, the velocity dispersion is ~ 200 km/s in the vicinity of our solar system).

We modeled the clumpy halo following Blasi and Sheth (2000) where they fit the simulations to a joint distribution of clump mass, m, and position, r, by

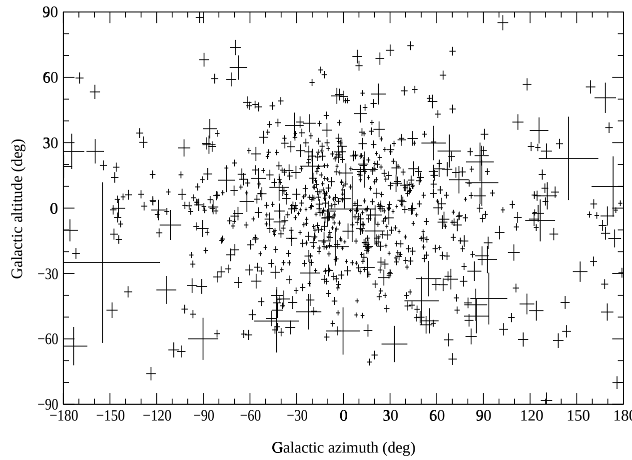

Fig. 1. Locations for 754 dark matter clumps with fluxes higher than CMB anisotropies between 1 and 1000 GHz. This realization of the Galactic halo follows a NFW profile and contains 3972 total clumps with $M_{cl} \geq 10^7 M_\odot$. Crosses represent the solid angle of each clump (multiplied by a factor of 5) inside which 90% of the flux is located.

$$n_{cl}(r,m) = n_{cl,0}\left(\frac{m}{M_H}\right)^{-\alpha}\left[1+\left(\frac{r}{r_c^{cl}}\right)^2\right]^{-3/2}\,, \tag{3}$$

where $n_{cl,0}$ is a normalization constant, r_c^{cl} is the core of the clumps distribution, and $\alpha \sim 1.9$ fits well the simulations in Ghigna et al. (1998). In Ghigna et al. (1998), a halo with $M_H \approx 2\times10^{12}\ M_\odot$ contains about 500 clumps with mass larger than $M_{cl} \sim 10^8\ M_\odot$. We present here the results for the case of dark matter halos following a NFW profile while other cases are considered in detail in Blasi, Olinto and Tyler (2001). The density of each clump is taken to be as in Eq. (2), where the normalization constant is calculated from the total mass, the core radius of the clump is assumed to be 0.1 of the clump radius and the latter is taken from the condition that the clump density equals the local density of dark matter in the Galaxy at the clump position.

We simulated several realizations of a clumpy halo each with about 4000 clumps of masses $M_{cl} \geq 10^7 M_\odot$. Figure 1 shows one realization with 3972 clumps in Galactic coordinates. Here we adopt a cross section for neutralino annihilation $\langle\sigma v\rangle_{\chi\bar{\chi}} = 3\times10^{-29}\,\mathrm{cm}^3/\mathrm{s}$. The results can be rescaled for the present choice of dark matter density profile (but this rescaling is not generic, see Blasi, Olinto and Tyler (2001)).

In Figure 1, 754 clumps have synchrotron fluxes in the range 1 to 1000 GHz above 10^{-5} times the CMB flux. These clumps are potentially detectable by anisotropy experiments where the isotropic CMB emission is subtracted and only anisotropies at the level of 10^{-5} times the CMB flux remain. Of these, 132 are above 30 degrees Galactic latitude (or below -30). The clumps range in angular sizes from the size of a pixel (10'x10') to about 10 degrees, occupying 2% of the solid angle of the sky. The crosses shown in the figure represent the solid angle (amplified by a factor of 5 for

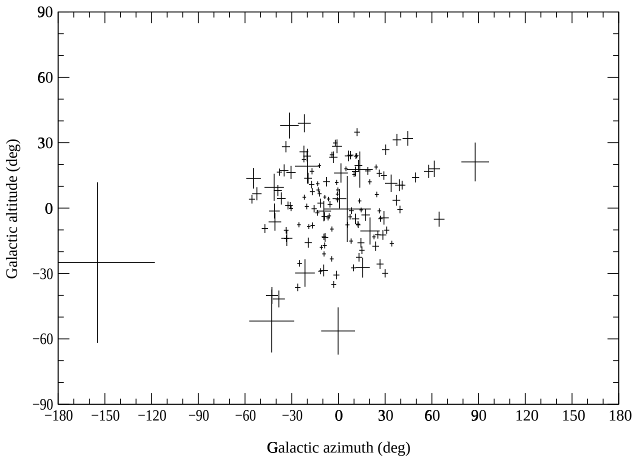

Fig. 2. Same as Fig. 1 but for observable clumps with fluxes higher than CMB anisotropies between 10 and 400 GHz.

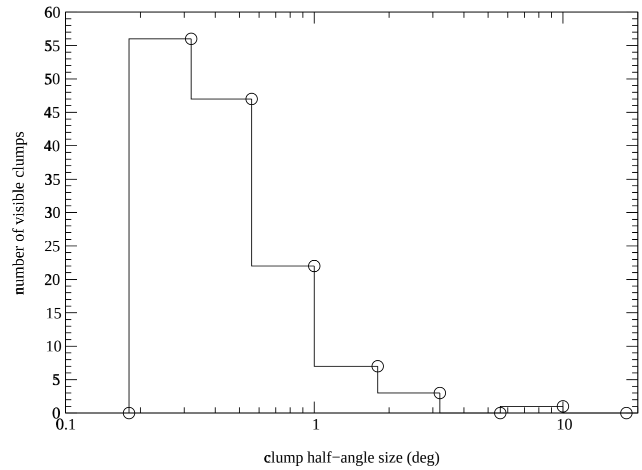

Fig. 3. Number of clumps of each angular size with fluxes above CMB anisotropies between 10 and 400 GHz.

clarity) inside which 90% of the radiation for each clump is located. Figure 2 shows the location and solid angles of clumps that are observable between 10 and 400 GHz. This range is expected to be relatively quiet of CMB foregrounds (see, e.g., Tegmark et al. (2000)), therefore the most sensitive CMB anisotropy experiments are planned for this range in frequency.

The histogram in Fig. 3 shows the number of observable clumps of different solid angles. There are over 100 clumps that can be observed by experiments with angular resolution around 0.2 degrees. A few very large objects can be seen even by experiments with poor angular resolution. These correspond to clumps located close to Earth. If a large object is identified in this frequency range, a spectral study would verify its nature as a dark matter clump. In addition, the radial dependence of the flux within the clump could further constrain CDM clustering behavior.

Figure 4 shows a histogram of the number of observable clumps with total flux in or above a given energy bin. The histograms in Figs. 3 and 4 were generated for the same realization in Fig. 1. For different realizations see Blasi, Olinto and Tyler (2001). The behavior shown in these figures is generic and can act as a guide to determine if microwave sources are annihilating dark matter clumps or some other foreground.

As an example of the spectral dependence of the synchrotron emission from WIMP annihilation, we show in Figure 5 the spectrum of a dark matter clump (thick line) compared with the CMB anisotropies (thin line) in the same solid angle occupied by the clump. This clump is chosen to lie at galactocentric coordinates [-4,0,0] kpc (where the Sun is located at [-8.5,0,0]), with $10^8 M_\odot$, occupying a half-angle of 1 degree on the sky. The neutralino mass was chosen to be 100 GeV. The dashed line shows the case of a neutralino with 10 TeV for comparison. The cutoff is moved to higher frequencies as expected from Eq. (1). If an annihilating dark matter clump were to be observed, the cutoff would give us the neutralino mass directly. The dotted line shows the flux for the same clump with $m_\chi = 100$ GeV but with the interaction strength, given by the WIMP annihilation cross section times velocity, $\langle\sigma v\rangle_{\chi\bar{\chi}}$, increased by a factor of 100.

3 Conclusions

The clumpy nature of CDM halos can be used to detect and constrain WIMP candidates for the non-baryonic dark matter. Neutralino annihilation in the higher density clumps can be observed via the synchrotron radiation of electrons and positrons as these annihilation products radiate in the Galactic magnetic field. The spatial structure of the Galactic magnetic field implies that the synchrotron emission from annihilation gets stronger as clumps get closer to the Galactic plane. This behavior gives a different angular distribution than the distribution from the gamma ray signature of the same clumps. This unique combination will help distinguish WIMP clumps from other extragalactic gamma ray sources. The frequency range where these clumps are better observed overlaps with highly sensitive experiments planned for CMB anisotropy measurements. The possibility of detecting these clumps will be soon within reach. Depending on the density profile of dark matter clumps, hundreds of clumps have detectable fluxes and angular sizes. Even more clumps may be present if the lower limit on clump masses is lowered from $10^7 M_\odot$.

The spectral shape, spatial distribution, and angular size of annihilating neutralino clumps discussed above represent some particular choices of m_χ and $\langle\sigma v\rangle_{\chi\bar{\chi}}$ which are hard to constrain a priori. The neutralino mass sets the cutoff of the spectrum and changes the overall flux while the cross section mostly influences the flux amplitude. Finally, the Galactic magnetic field structure above and below the plane of the Galaxy is poorly known and will also influence the exact observable clump distribution. The best strategy is to search for varying sizes of CMB foregrounds at a number of frequencies and select for those with the spectral dependence given

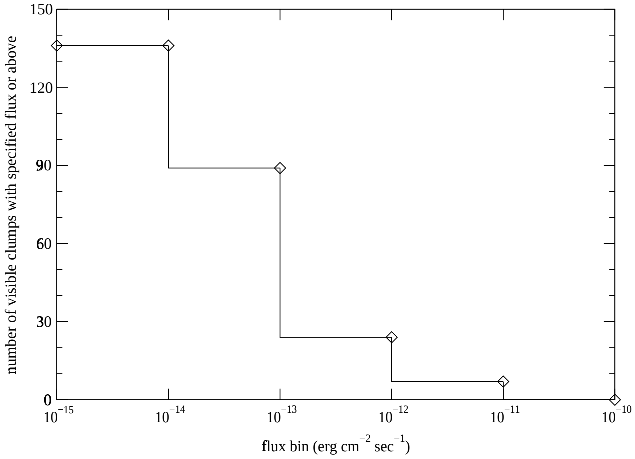

Fig. 4. Number of observable clumps with total flux in the specified flux bin or above.

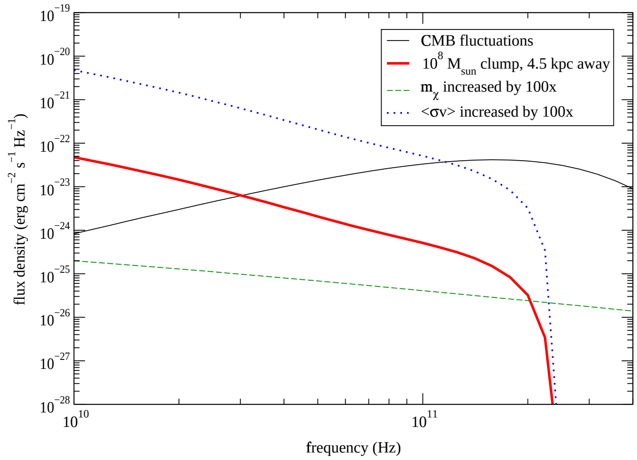

Fig. 5. Spectrum of synchrotron emission from an example NFW dark matter clump with $m_\chi = 100$ GeV (thick line) compared with the CMB anisotropies (thin line) in the same solid angle occupied by the clump. This clump is chosen to lie at galactocentric coordinates [-4,0,0] kpc, with $10^8 M_\odot$, occupying a half-angle of 1 degree on the sky. The flux from the same clump but with $m_\chi = 10$ TeV is represented by the dashed line and the dotted line is for $m_\chi = 100$ GeV and $\langle\sigma v\rangle_{\chi\bar{\chi}}$ increased by a factor of 100.

in Fig. 5. Once some extended synchrotron sources have been selected, the particular radial distribution and flux shape will help determine if these sources are dark matter clumps. The combination of these synchrotron measurements with the direct gamma ray and neutrino signature will make these sources unique. In addition, the synchrotron signature will help determine the structure of the magnetic field above the Galactic disk.

Future CMB experiments such as MAP and Planck can be used in conjunction with future gamma ray and neutrino experiments. Full sky coverage helps this determination since the Galactic plane is usually avoided by small area experiments. MAP will observe above about 20 GHz while Planck should start at 30 GHz, with a large increase in angular resolution that makes these objects easier to detect.

Acknowledgements. This work was supported by the NSF through grant AST-0071235 and DOE grant DE-FG0291 ER40606 at the University of Chicago, and at Fermilab by DOE and NASA grant NAG 5-7092.

References

Berezinsky, V., Gurevich, A.V., and Zybin, K.P., Phys. Lett. B 294, 221, 1992.

Berezinsky, V., Bottino, A., and Mignola, G. Phys. Lett. B 325, 136, 1994.

Bergström, L., Edsjö, J., Gondolo, P., Ullio, P., Phys. Rev. D 59, 043506, 1999.

Blasi, P., and Sheth, R. K., Phys. Lett. B 486, 233, 2000.

Blasi, P., Olinto, A.V., and Tyler, C., in preparation.

Calcáneo–Roldán, C. and Moore, B., astro-ph/0010056.

Ghigna, S., Moore, B., Governato, F., Lake, G., Quinn, T., Stadel, J., MNRAS 300, 146, 1998.

Gondolo, P., preprint hep-ph/0002226.

Gondolo, P. and Silk, J., Phys. Rev. Lett. 83, 1719, 1999.

Jungman, G., Kamionkowski, M., and Griest, K., Phys. Rep. 267, 195, 1996.

Navarro, J.F., Frenk, C.S., and White, S.D.M., Ap. J. 462, 563, 1996; ibid. 490, 493, 1997.

Stanev, T. , Astrophys. J. 479, 290, 1997.

Tegmark, M., Eisenstein, D.J., Hu, W., and de Oliveira-Costa, A., Ap.J. 530, 133, 2000.